The EMBO Journal Vol.18 No.16 pp.4414–4423, 1999

Endostatin inhibits VEGF-induced endothelial cell migration and tumor growth independently of zinc binding

Noriko Yamaguchi[1], Bela Anand-Apte[2], Margaret Lee[1], Takako Sasaki[3], Naomi Fukai[1], Robert Shapiro[4], Ivo Que[5], Clemens Lowik[5], Rupert Timpl[3] and Bjorn R.Olsen[1,6]

[1]Department of Cell Biology, Harvard Medical School, Boston, MA 02115, [2]Department of Cell Biology (NC10), Cleveland Clinic Foundation, Cleveland, OH 44195, USA, [3]Max-Planck Institut für Biochemie, D-82152 Martinsried, Germany, [4]Center for Biochemical and Biophysical Sciences and Medicine and Department of Pathology, Harvard Medical School, Boston, MA 02115, USA and [5]Endocrinology and Metabolic Diseases, Leiden University Medical Center, 2300 RC Leiden, The Netherlands

[6]Corresponding author
e-mail: bjorn_olsen@hms.harvard.edu

Endostatin, produced as recombinant protein in human 293-EBNA cells, inhibits the migration of human umbilical vein endothelial cells (HUVECs) in response to vascular endothelial growth factor (VEGF) in a dose-dependent manner and prevents the subcutaneous growth of human renal cell carcinomas in nude mice at concentrations and in doses that are from 1000- to 100 000-fold lower than those previously reported. The inhibition of migration is not affected by mutations which eliminate Zn or heparin binding and inhibition of tumor growth does not depend on Zn binding. The results of the migration assays suggest that endostatin causes a block at one or more steps in VEGF-induced migration, while VEGF in turn can cause a block of the inhibition by endostatin of VEGF-induced migration of HUVECs.

Keywords: angiogenesis/endostatin/heparin binding/tumor growth/zinc binding

Introduction

Collagen XVIII contains multiple triple-helical domains and serves as the core protein of a heparan sulfate proteoglycan in basement membranes (Oh *et al*., 1994a; Muragaki *et al*., 1995; Rehn and Pihlajaniemi, 1995; Halfter *et al*., 1998; Saarela *et al*., 1998). Proteolytic processing of the non-triple-helical C-domain (NC1) leads to release of heparin-binding fragments. One of these, the 22 kDa angiogenesis inhibitor endostatin, was initially purified from conditioned media of murine hemangioendothelioma cells based on its ability to inhibit the proliferation of bovine vascular endothelial cells *in vitro* (O'Reilly *et al*., 1997). *Escherichia coli*-derived recombinant endostatin was subsequently shown to induce regression and prevent growth of experimental tumors in mice when administered in daily doses as high as 20 mg/kg (Boehm *et al*., 1997; O'Reilly *et al*., 1997).

Endostatin was recently isolated as a soluble protein in human embryonic kidney cells expressing Epstein–Barr virus nuclear antigen-1 (293-EBNA) (Sasaki *et al*., 1998) and its crystal structure was determined (Hohenester *et al*., 1998). Studies of the domain structure, binding properties and protease sensitivity of the NC1 region of collagen XVIII (Sasaki *et al*., 1998) demonstrated that it consists of a trimerization region, a protease-sensitive segment and the endostatin domain. Both NC1 and endostatin bind to heparin, but in solid-phase binding assays NC1 bound to sulfatides and the basement membrane components perlecan and laminin-1 with half-maximal binding at 0.1–1 nM while endostatin was 100-fold less active (Sasaki *et al*., 1998).

Previous reports have suggested that proteolytic cleavage of collagen XVIII and exposure of a new N-terminal sequence is necessary for the formation of a biologically active molecule, and that coordination of a Zn atom in the N-terminal region of endostatin may be essential for this activity (O'Reilly *et al*., 1997; Boehm *et al*., 1998; Ding *et al*., 1998). To test these ideas and understand better how endostatin regulates the behavior of endothelial cells, we have examined the effects of recombinant human and mouse endostatins on migration of endothelial cells in response to the chemotactic inducer vascular endothelial growth factor (VEGF) and the ability of endostatins to affect the progression of a human renal carcinoma in nude mice. Surprisingly, the results demonstrate that not only endostatin, but also NC1 and endostatins with oligopeptide epitopes at the N- or C-termini inhibit endothelial cell migration in response to VEGF at picomolar concentrations. This activity does not depend on heparin binding or the N-terminal Zn-binding region of the molecule, but is critically dependent on the order in which the cells are exposed to endostatin and VEGF. The recombinant human and mouse endostatins and mutant endostatin with no Zn binding also induce regression and inhibit the subcutaneous growth of human renal carcinoma tumors in nude mice in daily doses at the nanogram level. The finding that endostatin can inhibit VEGF-induced migration of human umbilical vein endothelial cells (HUVECs) *in vitro* and inhibits the growth of a human renal carcinoma *in vivo* at levels that are 1000–100 000-fold lower than previously reported has obvious implications for the design of future clinical trials in humans.

Results

Production and purification of wild-type and mutant endostatins

We generated constructs for expression of human endostatin and NC1 in 293-EBNA cells with and without the oligopeptide epitope of influenza virus hemagglutinin (*flag*) at the N- or C-terminal ends (Figure 1A). Also, we

expressed three deletion mutants (Figure 1A) and several murine mutants in which specific arginyl residues were replaced by alanines (see below).

All purified recombinant proteins, except NC1, migrated on SDS–PAGE as single bands of the molecular weights expected (Figure 1B and C). Based on the yield of purified proteins, we estimate that culture media contain at least 3 mg/l of recombinant protein. On the gels, 50 ng of purified proteins were easily visualized. In contrast, when 30 or 200 μl of culture media from non-transfected 293-EBNA cells were analyzed by SDS–PAGE (Figure 1B), no endostatin band was observed by staining or Western blotting, suggesting that the endogenous production of collagen XVIII/endostatin by 293-EBNA cells is negligible compared with the level of recombinant proteins.

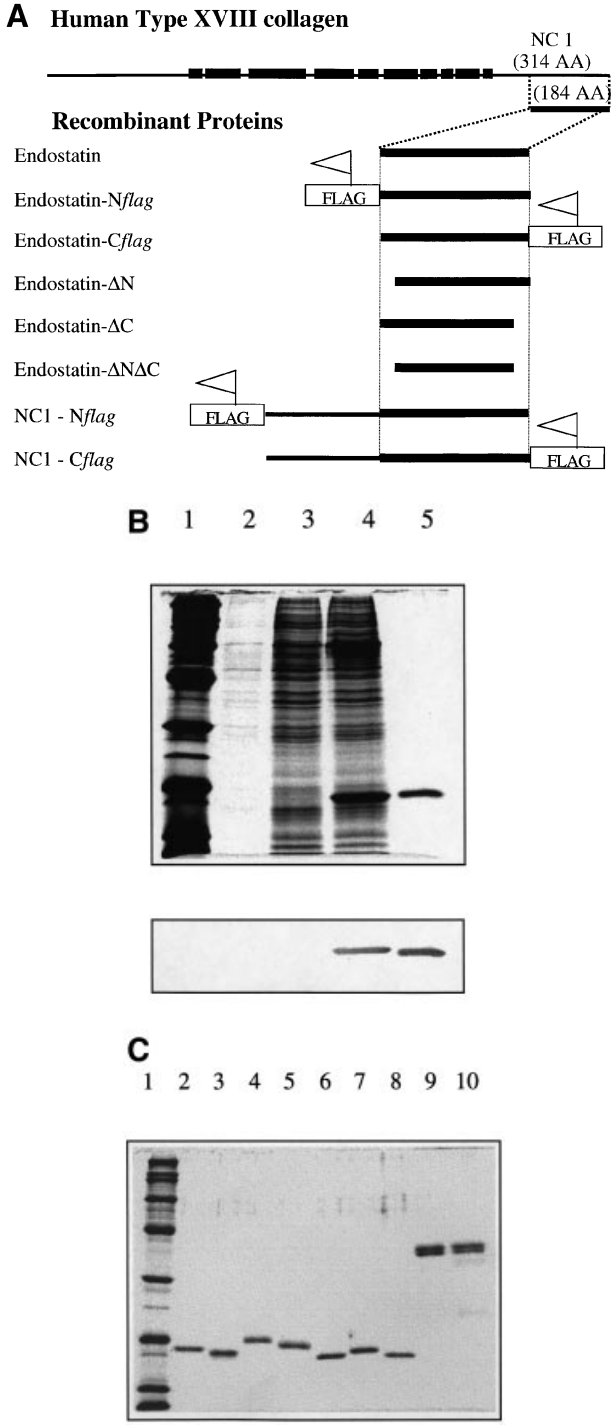

Endostatin inhibits migration of HUVECs in response to VEGF

In experiments designed to compare recombinant endostatin produced by 293-EBNA cells with recombinant endostatin produced by insect cells, we initially tested the ability of endostatins to inhibit basic fibroblast growth factor (bFGF)-stimulated proliferation of bovine capillary endothelial cells (O'Reilly *et al*., 1997), this being the assay initially used to detect endostatin activity in conditioned media of tumor cells. Unfortunately, the results were variable and inconsistent, even with cells prepared by the same laboratory in which the anti-angiogenic activity of endostatin was first discovered. Experiments with additional cells, including HUVECs and human dermal microvascular endothelial cells, did not show an effect on proliferation with any endostatin preparation and at concentrations as high as 1 μg/ml (data not shown). We therefore concluded that although proliferation assays were initially successful in identifying endostatin activity (O'Reilly *et al*., 1997), their lack of reproducibility make them unsuitable for *in vitro* studies of the structural requirements for the activity of endostatin. As a substitute for proliferation assays we turned to migration assays. In preliminary experiments it was observed that recombinant endostatin inhibited bFGF-induced migration of human dermal microvascular endothelial cells in a dose-dependent manner, with a half-maximal inhibitory concentration (IC_{50}) of 3 nM (data not shown). In subsequent experiments with HUVECs we found that endostatin had an even more potent inhibitory effect on migration in response to VEGF, with IC_{50} in the picomolar range (see below). The migration response of the cells was better with VEGF than bFGF (data not shown), consistent with previous findings (Yoshida *et al*., 1996), and the response to endostatin was maximal when the cells were subcultured to passages P4–P8. When cells were tested outside their optimal range of passages, we found reduced, or in some cases, no inhibition by endostatin, although the cells responded well to VEGF (data not shown).

We therefore chose to use VEGF-induced migration of HUVECs, subcultured to passages P4–P8, in experiments

Fig. 1. (**A**) Diagram showing the relative position of endostatin within the C-terminal NC1 domain of collagen XVIII and the various constructs used for expression of human recombinant proteins in 293-EBNA cells. (**B**) Coomassie-stained SDS–PAGE (top) and Western blot (bottom) of media from 293-EBNA cells.
Lane 1, molecular weight marker proteins; lane 2, 30 μl of 293-EBNA conditioned medium; lane 3, 200 μl of 293-EBNA conditioned medium; lane 4, 200 μl of conditioned medium of 293-EBNA cell expressing human endostatin; lane 5, 400 ng of purified recombinant human endostatin. Western blotting shows reactivity with polyclonal anti-endostatin antibodies only in lanes 4 and 5. (**C**) Coomassie-stained SDS–PAGE of purified recombinant proteins.
Lane 1, molecular weight marker proteins; lane 2, mES; lane 3, hES; lane 4, hES-N*flag*; lane 5, hES-C*flag*; lane 6, hES-ΔN; lane 7, hES-ΔC; lane 8, hES-ΔNΔC; lane 9, hNC1-N*flag*; and lane 10, hNC1-C*flag*. Three to four hundred nanograms of protein were loaded in each lane. Both bands within the doublet seen in NC1 preparations were positive in Western blots with anti-*flag* antibodies (data not shown). We believe therefore that the doublet is due to post-translational modification or an internal folding effect.

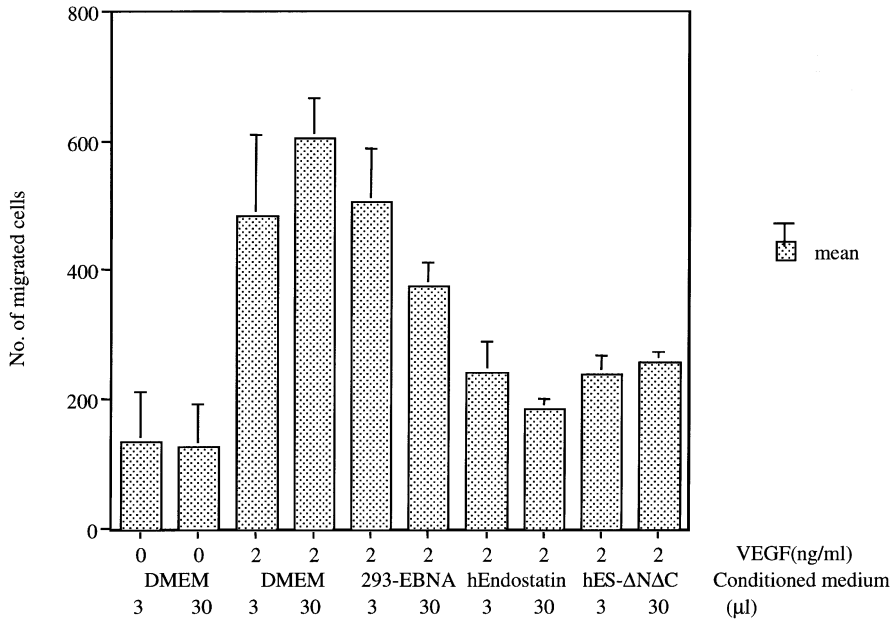

Fig. 2. The results of migration assays with 2 ng/ml of VEGF as chemotactic inducer and preincubation of HUVECs for 30 min with different amounts of medium (DMEM), conditioned medium from 293-EBNA cells, conditioned medium from cells expressing human endostatin, and conditioned medium from cells expressing human endostatin with both amino and carboxyl pentapeptide segments deleted (hES-ΔNΔC).

aimed at defining the structural requirements for the activity of endostatin *in vitro*. When VEGF was used at a concentration of 2 ng/ml in the lower chamber, and 3 or 30 μl of conditioned medium from human endostatin-producing 293-EBNA cells were preincubated with cells in the upper chamber, migration of cells through the collagen I-coated polycarbonate filter was almost completely inhibited (Figure 2). In contrast, 3 and 30 μl of medium alone [Dulbecco's modified Eagle's medium (DMEM)] or conditioned medium from mock-transfected 293-EBNA cells had no or minimal effects. *Flag*-containing endostatins and NC1 were as effective inhibitors of migration as endostatin without the *flag* sequence (Figure 3A); *flag*-containing proteins that had been purified on an anti-*flag* antibody column were also fully active (data not shown). As little as 0.1 ng/ml of purified recombinant human endostatin inhibited the migration of cells through the filter (Figure 3B). In the absence of VEGF, endostatin had no effect on migration (Figure 3B). The high degree of sensitivity of HUVECs to endostatin was evident from dose–response experiments: half-maximal response to endostatin was seen with 1.3 pM (Figure 4A). For NC1-C*flag* the IC_{50} was also 1.3 pM.

The migration response was critically dependent on preincubation of the cells with endostatin. When endostatin was added directly to cells in the upper chamber at the beginning of the migration assay, no inhibition was observed although endostatin was present during the entire 6-h incubation period of the assay (Figure 4B). Also, preincubating the HUVECs with endostatin for 10 min before the cells were added to the upper chamber was not sufficient to produce an inhibitory effect. Preincubation of cells with endostatin for 30 min, however, produced inhibition of migration to background levels, even when cells were washed before they were tested (Figure 4B).

Inhibition of migration by mutant endostatins

To determine whether Zn binding is important for the inhibitory activity we tested recombinant endostatins that lacked the N- and/or C-terminal pentapeptide sequences. Endostatin contains 1 mol of Zn per mol of protein; endostatins with N-terminal deletions contained no Zn (Table I). In contrast, mutant endostatin with only the C-terminal pentapeptide sequence deleted contained the same amount of Zn as wild-type endostatin. In the migration assays (Figures 2 and 5A), all three deletion mutants showed the same inhibitory activity as endostatin; the dose–response curve for the double-mutant was similar to that of wild-type endostatin and the IC_{50} was 1.3 pM. Endostatins with the N-terminal or N- and C-terminal pentapeptides deleted had identical N-terminal sequences, APLAFQPVLH---, while the mutant with only the carboxyl sequence missing had the wild-type sequence APLAHSHRDFQP---. In both sequences the APLA residues are derived from the signal peptide in the expression vector (Mayer *et al*., 1993).

We also tested mutants in which specific arginyl residues were replaced by alanines. As predicted, mutation of arginines within a large basic patch on one side of the endostatin structure (Hohenester *et al*., 1998) resulted in proteins that eluted from heparin columns by lower concentrations of NaCl than wild-type protein, but there was no correlation between inhibitory activity in the migration assay and heparin binding (Figure 5B). In addition, the dose–response curve for a mutant in which two arginines (R158 and R270) were replaced by alanines, was nearly identical to that of wild-type endostatin with IC_{50} being 3 pM.

Anti-tumor activities of mutant endostatin with no zinc binding

To test the biological activity of mutant endostatin with no Zn binding *in vivo*, we compared wild-type endostatin

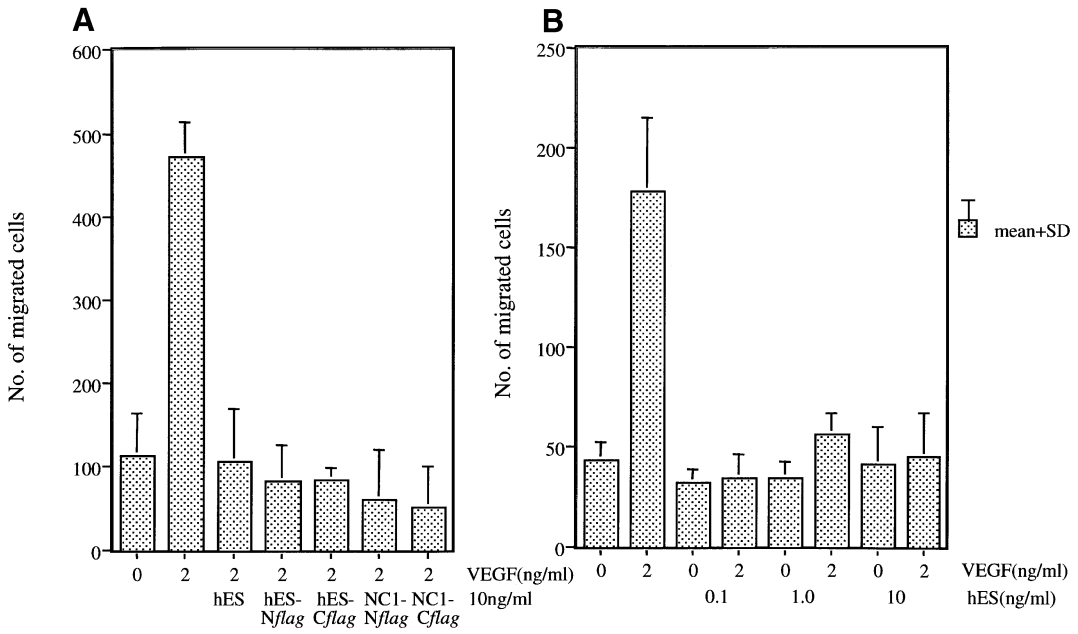

Fig. 3. (**A**) The results of migration assays with 2 ng/ml of VEGF and preincubation of HUVECs for 30 min with 10 ng/ml of human endostatin (hES), hES-N*flag*, hES-C*flag*, NC1-N*flag* and NC1-C*flag*. At this concentration all recombinant proteins showed inhibition of migration to background levels. (**B**) The results of migration assays with 30 min preincubation of HUVECs with 0.1–10 ng/ml of human endostatin. Note that endostatin had no effect on random migration through the filter in the absence of VEGF.

and mutant protein lacking both N- and C-terminal pentapeptides in a tumor progression assay. When a human kidney carcinoma (RC-9) was grown subcutaneously in nude mice, wild-type human endostatin caused tumor regression and slowed further growth during a 2-week period when injected daily at doses of 10–250 μg/kg around the tumor. Beyond 2 weeks, a rebound effect was seen at the higher doses, but this effect was relatively insignificant at 10 μg/kg (Figure 6A). For all dose levels of endostatin injected, however, tumor regression took place during the first 4 days after the initial injection (Figure 6B). Therefore, to compare the ability of wild-type endostatin and mutant endostatin with no Zn binding to affect tumor progression *in vivo*, we examined regression of RC-9 tumors during 4 days of treatment. As can be seen in Figure 7A, both wild-type and mutant endostatins caused the same degree of regression when injected daily at a dose of 10 μg/kg around the tumor. In contrast, tumors continued to grow in control mice that were injected with physiological saline without endostatin (Figure 7A). The RC-9 tumor produces interleukin-6 and parathyroid hormone-like protein (PTHrP) and therefore causes hypercalcemia and hypophosphatemia (Weissglas *et al*., 1995, 1997). As expected, when serum levels of calcium and phosphate were determined at the end of the experiment, endostatin-treated animals had lower calcium levels and higher phosphate levels than animals in the control group (Figure 7B and C).

Discussion

Recombinant endostatin produced in 293-EBNA cells

We demonstrate here that 293-EBNA cells can be used to produce endostatins with high levels of biological activity. Although it is possible that 293 cells synthesize and secrete collagen XVIII and proteolytic fragments such as endostatin, the endogenous level is insignificant when compared with the levels obtained for recombinant proteins (Figures 1B and 2). Also, *flag*-containing endostatin purified on an anti-*flag* column was as effective an inhibitor of endothelial cell migration as endostatin purified by heparin chromatography. We conclude therefore that the biological effects we describe are not caused by endogenous factors secreted by 293-EBNA cells.

Recombinant endostatins inhibit migration of HUVECs

The choice of VEGF-induced migration of HUVECs as an *in vitro* assay to examine the structural requirements for the activity of endostatin was based on our inability to consistently reproduce endostatin effects in endothelial cell proliferation assays (see above). It was also dictated by previous work showing that while VEGF was a strong inducer of chemotactic migration of HUVECs at concentrations of 1–10 ng/ml, bFGF was mostly a stimulator of chemokinesis at concentrations of 10–100 ng/ml (Yoshida *et al*., 1996). Finally, known inhibitors of angiogenesis, such as α-interferon, platelet factor 4 and TNP-470, inhibit migration as well as proliferation of HUVECs (Yoshida *et al*., 1996). Thus, we concluded that VEGF-induced migration of HUVECs was an excellent alternative to proliferation assays for comparing the anti-angiogenic activities of wild-type and mutant endostatins.

The results reported here support this conclusion. Not only do various endostatins inhibit VEGF-induced HUVEC migration at picomolar levels, but these inhibitory activities are also reflected in the abilities of wild-type and mutant endostatin with no Zn binding to inhibit tumor progression at the corresponding low daily doses. The ability of endostatins with or without *flag*-epitopes to

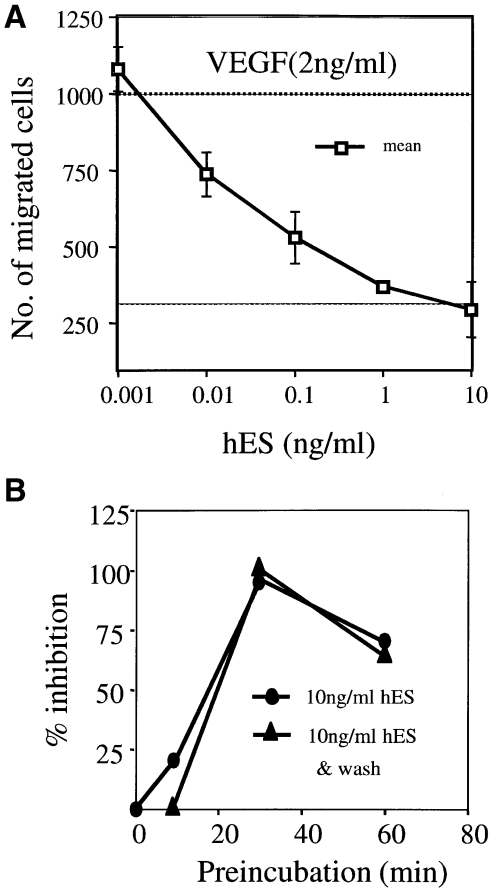

Fig. 4. (**A**) The results of migration assays with various concentrations of human endostatin. The number of migrated cells in the absence and presence of 2 ng/ml of VEGF in control chambers are indicated by the dotted lines. (**B**) The effect of preincubation of HUVECs with human endostatin (hES) before the cells were loaded into the upper chamber of the migration apparatus. After preincubation for the times indicated, the cells were loaded either with hES (●) or washed, resuspended in fresh medium and loaded without hES (▲).

Table I. Zinc content of endostatin and deletion mutants

Sample	[Zn], μM	[Protein], μM	Zn/protein molar ratio
hES	15.3/7.41	16.2/7.7	0.94/0.96
hES-ΔNΔC	0.3/0.44	11.2/6.4	0.03/0.07
hES-ΔN	0.3/0.68	7.6/4.3	0.04/0.16
hES-ΔC	10.9/5.00	9.6/5.0	1.14/1.00

Zinc concentrations were measured by flame atomic absorption spectrometry with a Perkin Elmer 2280 instrument. The two sets of numbers in each column are measurements with two different preparations of endostatin and endostatin deletion mutants. One preparation was derived from conditioned medium stored in 2.5 mM EDTA; the second preparation had not been exposed to EDTA. In control experiments we measured the zinc concentrations of PBS, to which samples were dialyzed before analysis.

inhibit VEGF-induced migration of HUVECs in the 0.05–500 pM range (Figure 4A), however, is remarkably different from what has been reported by others. Dhanabal *et al*. (1999) reported inhibition of ECV304 cell migration in response to bFGF with 20 μg/ml of *Pichia pastoris*-produced endostatin, while our results show complete inhibition at 10 000–100 000-fold lower concentrations.

One potential explanation for this dramatic difference in activity could be an inherent difference between endostatin from 293-EBNA cells and *Pichia*. The 293-derived material crystallized readily and provided the first crystal structure of endostatin (Hohenester *et al*., 1998). In contrast, although *Pichia*-derived protein has been reported to migrate as a single band on SDS–PAGE (Dhanabal *et al*., 1999), no data were available to assess whether the material is properly folded. Also, while the 293-EBNA cell-derived endostatin induces regression of a renal carcinoma tumor grown in mice at doses of 10 μg/kg/day, *Pichia* endostatin was reported to be effective in preventing growth of a renal clear cell carcinoma in mice at doses of 10 mg/kg/day. Although these reported results are different from ours, we do believe, however, that *Pichia*-derived recombinant endostatin is quite similar to that produced by 293-EBNA cells. There is no evidence for post-translational modification of endostatin by 293-EBNA cells (Sasaki *et al*., 1998) and the cDNA constructs used for expression in *Pichia* and 293-EBNA cells all have the same origin (Oh *et al*., 1994b), so the expressed proteins should have identical sequences. Also, in a direct comparison of *Pichia*-derived human endostatin (provided by EntreMed, Inc.) with that produced by 293-EBNA cells, the inhibitory effects on VEGF-induced migration of HUVECs were quite similar (data not shown). Therefore, we believe that the difference between the results reported by Dhanabal *et al*. (1999) and the results reported here are unlikely to be explained by a major difference between the recombinant endostatins used.

A second and more likely possibility is that ECV304 cells may be less sensitive to endostatin than HUVECs. While we rejected ECV304 cells for our assays because of their poor response to VEGF, inhibition of migration with *Pichia*-derived endostatin at 20 μg/ml levels was demonstrated with such cells by Dhanabal *et al*. (1999). The reason for the poor response to VEGF and endostatin by ECV304 cells may well be that these cells, previously assumed to represent transformed HUVECs and utilized in a large number of studies, have recently been shown to be derived from the bladder carcinoma cell line T24 (see ATCC at http://www.atcc.org). The effects of endostatin on ECV304 cells (Dhanabal *et al*., 1999) may therefore be more typical for effects on a non-endothelial cell than specific effects on endothelial cells. Also, sensitivity to endostatin is determined significantly by whether the cells are in contact with endostatin before they are exposed to the chemotactic inducer. As demonstrated in Figure 4B, preincubation of HUVECs with endostatin for at least 30 min before exposure of the cells to VEGF is critical for an inhibitory effect on migration. Variations in preincubation time could therefore generate large differences in sensitivity and help explain differences between our results and those of other laboratories.

Zn binding is not critical for the inhibitory effects of endostatin on VEGF-induced migration and tumor growth in mice

Our results with mutations that abolish binding of Zn to endostatin are in sharp contrast to a recent report concluding that Zn binding is essential for the anti-angiogenic activity (Boehm *et al*., 1998). Not only do we find that endostatin with no Zn inhibits VEGF-induced HUVEC cell migration as effectively as wild-type endostatin

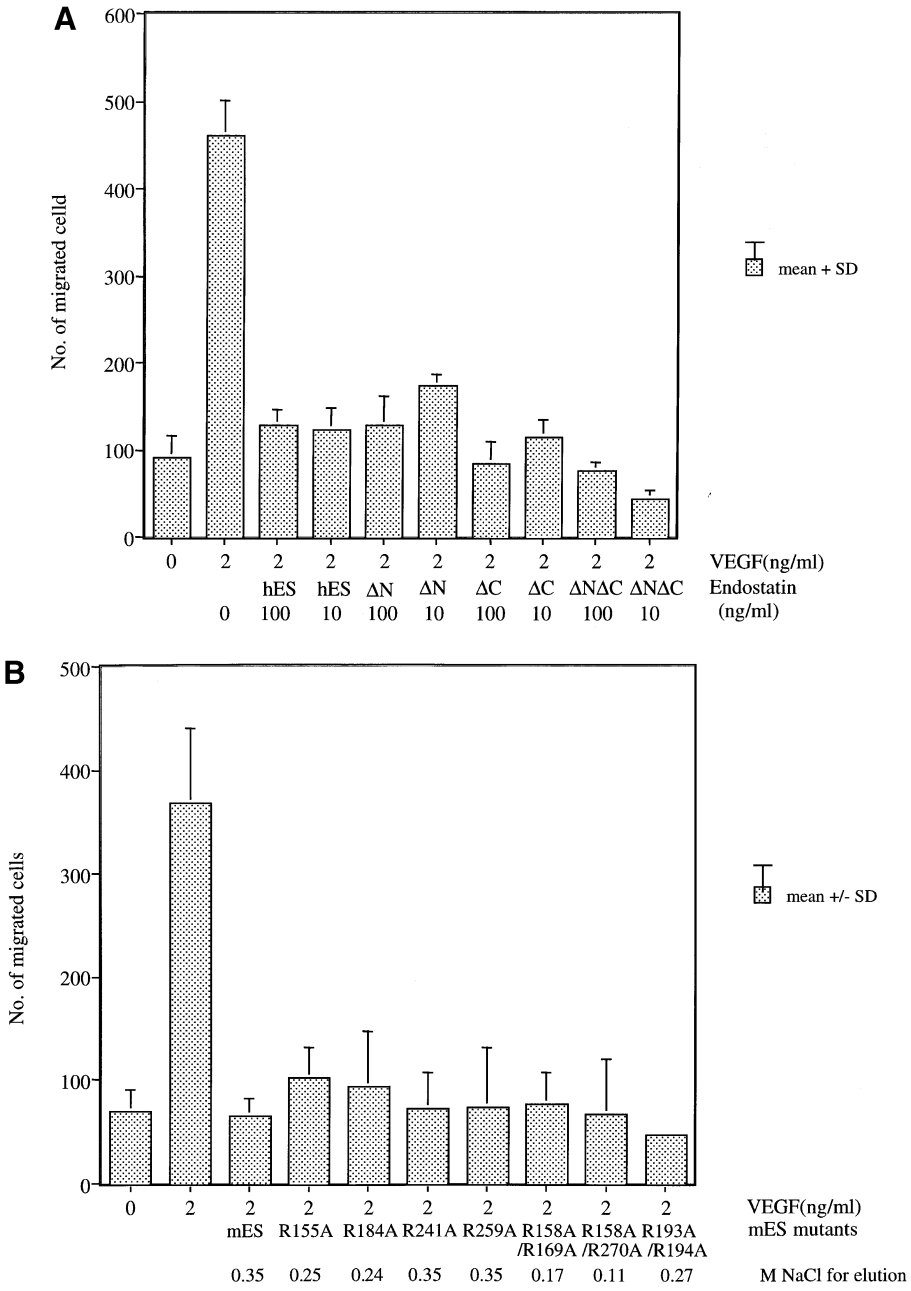

Fig. 5. (**A**) The results of migration assays with 2 ng/ml of VEGF and preincubation of HUVECs for 30 min with 10 ng/ml or 100 ng/ml of hES, hES-ΔN, hES-ΔC and hES-ΔNΔC. All recombinant proteins showed inhibition to background levels. (**B**) The results of migration assays with 2 ng/ml of VEGF and preincubation of HUVECs for 30 min with wild-type mouse endostatin (mES) or various murine mutants in which specific arginines were replaced by alanine residues. Below the diagram are indicated the concentrations of NaCl needed to elute the various proteins from analytical heparin columns.

(Figures 2 and 5A), but we also show that Zn-free endostatin causes regression of a renal carcinoma *in vivo* as effectively as Zn-containing endostatin (Figure 7). We believe that the apparent discrepancy between our conclusion and that of Boehm *et al*. (1998) may be due to differences in the recombinant proteins. The mutant proteins tested for biological activity by Boehm *et al*. (1998) were expressed in *E.coli* and represented an insoluble mixture of monomers and disulfide-linked oligomers of endostatin (see also Dhanabal *et al*., 1999). Since the oligomers are unlikely to have a perfectly folded structure (Hohenester *et al*., 1998), only the monomers are likely to refold into a native structure following injection into animals, and mutations that negatively affect refolding will cause a decreased biological activity *in vivo*. The decreased activity observed by Boehm *et al*. (1998) could therefore have been a refolding artefact and not an effect directly due to the lack of Zn binding.

Heparin binding is not essential for the ability of endostatin to inhibit VEGF-induced endothelial cell migration

We have previously demonstrated (Sasaki *et al*., 1998) solid phase binding of endostatin to major components of basement membranes, including the large heparan sulfate proteoglycan perlecan, at nanomolar concentrations. The

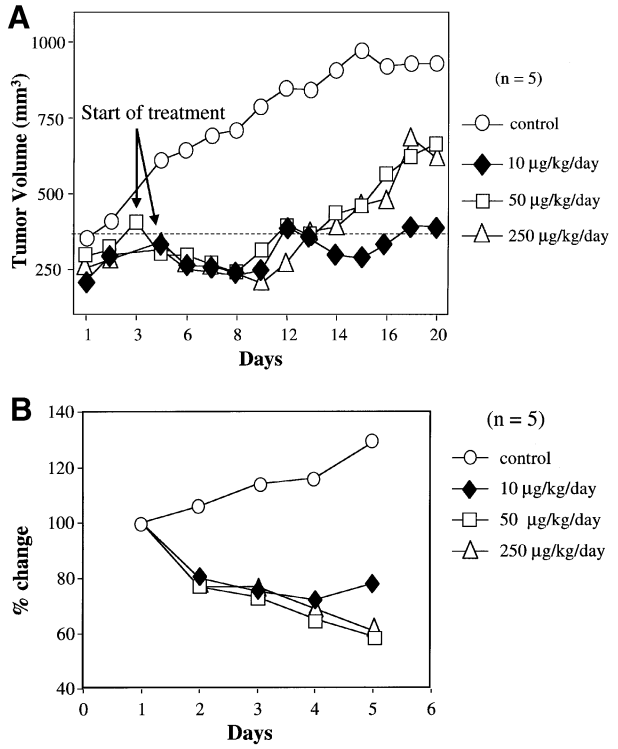

Fig. 6. (**A**) The effect of recombinant human endostatin on RC-9 tumor volume. RC-9 tumor-bearing mice (five animals per group) were treated for 16 or 17 days either with PBS or with 10, 50 or 250 µg/kg/day of endostatin. (**B**) Regression of RC-9 tumors during the first 4 days of treatment with recombinant human endostatin. Data shown in (A) expressed as % change for the first 4 days of treatment with endostatin.

strong inhibitory effect of mutants that have lost the ability to bind to heparin at physiological ionic strength, however, rules out an essential role for heparin binding in the inhibition of VEGF-induced migration. The use of heparin-binding mutants should simplify the study of other interactions between endostatin and cell surface structures which may be critical for the biological activity.

How does endostatin inhibit endothelial cell migration in vitro?

The mechanisms by which endostatin inhibits VEGF-induced cell migration are not known, but our data rule out some of the potential models. For example, the preincubation results (Figure 4B) provide a compelling argument against the possibility that endostatin interferes directly with binding of VEGF to its receptors. The presence of endostatin with the cells from the start of the migration assay and during the entire 6-h assay had no effect on migration, even at 100-fold higher concentrations than those needed for complete inhibition following a 30-min preincubation. Also, since preincubation of HUVECs with endostatin had no effect on the cell surface levels of immunoreactive VEGF receptors (data not shown), we can rule out the possibility that inhibition of migration is caused by an endostatin-induced decrease in the number of VEGF receptors. Therefore, we hypothesize that endostatin induces a block in one or more steps in VEGF-mediated cell migration. Since the presence of endostatin during the migration assay without the preincubation step has no effect on migration, it is likely that VEGF-induced migration in turn inhibits the endostatin-inducible blocking mechanism.

How does endostatin work in vivo?

Endostatin exerts an inhibitory effect on VEGF-induced cell migration *in vitro* at picomolar concentrations. Given the inhibitory effects on tumor progression in nude mice seen with daily doses as low as 10 pmol (200 ng) of recombinant protein (Figures 6 and 7), it is possible that inhibition of endothelial cell migration (and, as a consequence, angiogenesis) may be responsible for the *in vivo* effects as well. Obviously, we cannot rule out the possibility that other effects of endostatin may contribute to the effects *in vivo*. In future studies it would be important to analyze the *in vivo* effects of recombinant endostatins on other aspects of angiogenesis, such as endothelial cell proliferation, tube formation and apoptosis at concentrations similar to those demonstrated to be effective on migration in this study. Such additional effects may well explain why endostatin causes regression of RC-9 tumors *in vivo* within a short period of time while inhibition of VEGF-induced migration *in vitro* requires preincubation of cells for at least 30 min in the absence of VEGF. It is also possible that within the tumor the dynamic process of angiogenesis allows endothelial cells to be exposed to endostatin before they are activated via their VEGF receptors.

We selected the RC-9 tumor for the *in vivo* experiments because of the previous demonstration (Weissglas *et al*., 1995) that there is a correlation between tumor volume and serum calcium, phosphate and PTHrP levels due to the constitutive production of PTHrP by the tumor cells. Serum calcium and phosphate, therefore, reflect tumor cell activity and can be used as a marker apart from tumor volume to measure tumor regression or progression. The changes in serum calcium and phosphate (Figure 7) seen following even a brief endostatin treatment, suggest that the reduced tumor volume is due to a reduced tumor cell mass and not simply a reduction in tumor liquid or extracellular matrix. The effect, seen with daily doses of 10 µg/kg, occurs at a dose which is 1000-fold lower than previously reported (Dhanabal *et al*., 1999) for *Pichia pastoris* endostatin in another renal carcinoma model. The complete explanation for this difference in activity is not clear, but several factors could be important. These could include different sensitivities to endostatin by different tumor cells, as well as different modes of administration. Clearly, a systematic comparison of the effects of soluble recombinant endostatins (produced in *Pichia* or 293-EBNA cells) on a number of different kinds of tumors, including different modes of administration, would be of considerable importance since most published studies on the effects of endostatin on tumor progression in animals have utilized insoluble material recovered from inclusion bodies in *E.coli*. Such investigations are beyond the scope of the present study, but our results should be helpful in their design. Additional studies are also needed to confirm and understand the resumption of RC-9 tumor growth seen after ~2 weeks of treatment with the higher doses of endostatin. At present we have no explanation for this effect; several possible mechanisms need to be considered in further studies, including an escape of endothelial cells to other angiogenic pathways that are not sensitive to

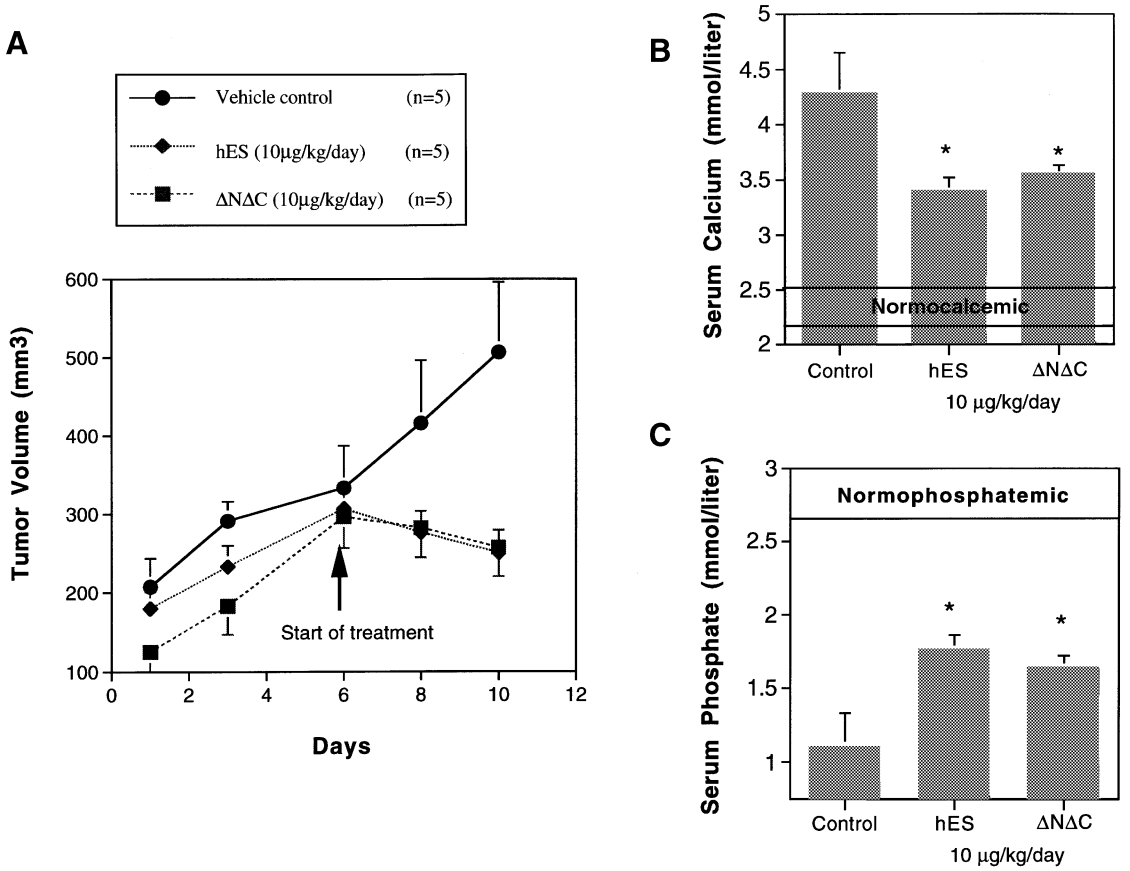

Fig. 7. (**A**) The effect of recombinant human endostatin (hES) and the double mutant (ΔNΔC) on RC-9 tumor volume. RC-9 tumor-bearing mice (five animals per group) were treated for 4 days either with PBS or with 10 μg/kg/day hES or ΔNΔC. (**B**) Effect of hES and ΔNΔC on serum calcium. After 4 days of treatment blood was taken and serum calcium was determined by automated autoanalyzer techniques. (**C**) Effect of hES and ΔNΔC on serum phosphate. After 4 days of treatment blood was taken and phosphate was determined by automated autoanalyzer techniques. Values are expressed as mean ± SEM. Differences between groups were examined by one-way ANOVA for multiple comparison followed by Fisher's test. *$p < 0.05$. In these mice normal serum calcium levels ranged between 2.1 and 2.5 mmol/l and serum phosphate between 2.7 and 3.0 mmol/l.

endostatin, an increase in an endostatin-binding protein that neutralizes its effects, or downregulation of molecules that are essential for the inhibitory effects of endostatin.

Materials and methods

Cell culture

HUVECs were purchased from Cascade Biologics, Inc. (Portland, OR) and grown in M200 medium, LSGS (low serum growth supplement), and 1% glutamine/penicillin/streptomycin (Irvine Scientific, Santa Ana, CA). Culture plates were coated with attachment factor (1% gelatin, Cascade Biologics, Inc.). Cells were cultured at 37°C and 5% CO_2. Only passages 4 to 8 were used. ECV304 cells were obtained from American Type Culture Collection (ATCC, Rockville, MD) and cultured in M199 medium containing 10% heat-inactivated fetal bovine serum (Summit Biotechnology, Ft Collins, CO) and 1% glutamine/penicillin/streptomycin.

Construction of expression vectors

Human α1(XVIII) cDNA clone pNF18-2 (Oh *et al*., 1994b) was used as template in the PCR to amplify sequences encoding endostatin (hES), endostatin-N*flag*, endostatin-C*flag*, NC1-N*flag*, and NC1-C*flag*. PCR was performed with Taq DNA polymerase (Qiagen, Chatsworth,CA) using the following oligonucleotide primers:

1. AGCGCTAGCTCACAGCCACCGCGACTTCCAGCCG
2. GTCGGCGGCCGCGGTGGCTACTTGGAGGCAGTCA
3. AGCGCTAGCTGACTACAAGGACGACGATGACAAGCACAGCCACCGCGACTTCCAGCCG
4. CAGCGCGGCCGCTCACTTGTCATCGTCGTCCTTGRAGTCCTTGGAGGCAGTCATGAAGCTGTT
5. AGCGCTAGCTGACTACAAGGACGACGATGACAAGTCAGGGCAGGTGAGGCTCTGGGCT
6. AGCGCTAGCTTCAGGGCAGGTGAGGCTCTGGGCT

The primers 1 and 2 were used for endostatin, 2 and 3 for hES-N*flag*, 1 and 4 for hES-C*flag*, 2 and 5 for NC1-N*flag*, and 4 and 6 for NC1-C*flag*. These primers contained the annealing sequences to cDNA, the *flag* peptide coding sequence Asp-Tyr-Lys-Asp-Asp-Asp-Asp-Lys (primers 3, 4, 5), and an *Nhe*I site at the 5′ end (primers 1, 3, 5) or a stop codon followed by a *Not*I site at the 3′ end (primers 2, 4, 6) to be inserted in frame with the BM-40 signal peptide (Mayer *et al*., 1993). The PCR products were ligated into pBluescript II SK(+) (Stratagene, La Jolla, CA). *Eco*RV, *Not*I sites, and insert sequences were confirmed by cycle sequencing (Ampli Cycle Sequencing kit; Perkin Elmer, Branchburg, NJ). All inserts were liberated by *Nhe*I and *Not*I digestion and cloned into the modified episomal expression vector pCEP-Pu (Kohfeldt *et al*., 1997). The deletion mutants of endostatin lacking five amino acids from the N- (His-Ser-His-Arg-Asp) or C-terminus (Met-Thr-Ala-Ser-Lys) were made as described above except that the PCR primers were as follows:

7. AGCGCTAGCTTTCCAGCCGGTGCTCCACCTGGTT
8. GTCGGCGGCCGCTAGAAGCTGTTCTCAATGCAGA

Primers 7 and 8 were used for the N-terminal deletion mutant (hES-ΔN) and the C-terminal deletion mutant (ES-ΔC), respectively. The mouse endostatin construct (mES) was described previously (Sasaki *et al*., 1998) and was used to introduce single or double mutations R155A, R184A, R241A, R259A, R158A/R169A, R158A/R270A, and R193A/R194A using corresponding pairs of oligonucleotides by fusion PCR (Vallejo *et al*., 1994; Pöschl *et al*., 1996).

Expression and purification of recombinant proteins

Human embryonic kidney cells (293-EBNA) expressing Epstein–Barr virus nuclear antigen (EBNA)-1, were purchased from Invitrogen

(Carlsbad, CA) and used for lipofectin-based transfection (Life Technologies, Gaithersburg, MD). Transfected cells were selected with 0.5 μg/ml of puromycin and serum-free conditioned medium was collected. Proteinase inhibitors were added to final concentrations of 2.5 mM EDTA, 1 mM *N*-ethylmaleimide and 2 mM phenylmethylsulfonyl fluoride. The conditioned medium was dialyzed against 0.02 M Tris–HCl pH 7.5, 0.15 M NaCl and applied to a Hi-trap heparin column (Pharmacia, Piscataway, NJ) which had been equilibrated with the same buffer. The recombinant proteins were eluted by a linear gradient of NaCl concentration from 0.15 to 0.8 M. Alternatively, hES-N*flag* and hES-C*flag* were purified on an anti-*flag* antibody column using Anti-*Flag* M2 affinity gel (Sigma, St Louis, MO). Conditioned medium containing *flag*-tagged endostatin was dialyzed against 0.05 M Tris–HCl pH 7.5, 0.15 M NaCl and then applied to the column. Fusion protein was eluted with 0.1 M glycine–HCl pH 3.5 and neutralized with 1.0 M Tris–HCl pH 8.0 immediately after elution. Purified proteins were dialyzed against phosphate-buffered saline (PBS) or phosphate buffer containing 0.5 M NaCl.

The mouse endostatin arginine mutants were purified by chromatography on a heparin–Sepharose column equilibrated in 0.05 M Tris–HCl pH 7.4 followed by molecular sieve chromatography (Sasaki *et al*., 1998). The purified mutant proteins all showed in SDS–PAGE a single band with the mobility of mouse endostatin (data not shown). Concentrations of NaCl required to replace the mutants from an analytical heparin Hi-trap column were determined as described (Sasaki *et al*., 1998).

Protein sequencing, Zn analysis and gel electrophoresis

Protein sequencing was performed by the Molecular Biology Core Facility at the Dana-Farber Cancer Institute. An Applied 477 Pulsed Liquid Sequencer (Applied Biosystems, Foster City, CA) was used for automated Edman degradation and the cleaved amino acid derivatives were analyzed using an Applied Biosystems 120 A Analyzer.

The Zn content of endostatins was measured by flame atomic absorption spectrometry with a Perkin Elmer 2280 instrument. For the Zn determinations, protein concentrations were determined on a Biotronic LC3000 amino acid analyzer after hydrolysis with 6 N HCl (16 h, 110°C). For all other assays, protein concentrations were measured by the MicroBCA (Pierce, Rockford, IL) method.

The purity of the proteins used in the migration assays and injected into nude mice was analyzed by SDS–PAGE in 13.5% gels. The gels were stained with Silver Stain Plus or Coomassie Brilliant Blue R250 (both from Bio-Rad, Hercules, CA). Western blotting was carried out using polyclonal anti-endostatin antibodies described previously (Sasaki *et al*., 1998).

Migration assays

Migration assays were performed in a modified Boyden chamber using a 48-well chemotaxis chamber (Neuroprobe Inc., Gaithersburg, MD). Eight micron Nucleopore polyvinylpyrrolidine-free polycarbonate filters (Corning, Cambridge, MA) were coated with 100 μg/ml of collagen type I (Collaborative Biomedical Products, Bedford, MA) in 0.2 N acetic acid for 2 days and air dried. The filter was placed over a bottom chamber containing $VEGF_{165}$ (purchased from R & D systems, Minneapolis, MN and Collaborative Biomedical Products, Bedford, MA) in 0.1% bovine serum albumin (BSA) (7.5% BSA, Fr. V solution was obtained from Sigma, St Louis, MO) in M200 medium. HUVECs were suspended in M200 medium and 10 000 cells in 50 μl were added to each well in the upper chamber. For testing the inhibitory activity of recombinant proteins, HUVECs were preincubated with the proteins in M200 medium in the cell culture incubator for 0–60 min before being added to the upper chambers. The assembled chemotaxis chamber was incubated for 6 h at 37°C with 5% CO_2 to allow cells to migrate through the collagen-coated polycarbonate filter. Non-migrated cells on the upper surface of the filter were removed by scraping with a wiper tool (Neuro Probe, Inc., Gaithersburg, MD) and a cotton swab, and the filter was stained with Diff-Quick stain (VWR Scientific Products, Bridgeport, NJ). The total number of migrated cells with nuclei per well were counted; the assays were run in quadruplicate.

Renal cell carcinoma model

RC-9 is derived from a patient with renal cell carcinoma in the advanced stage which, when transplanted into nude mice, induces hypercalcemia and hypophosphatemia due to constitutive expression of PTHrP (Weissglas *et al*., 1995, 1997).

Selected RC-9 tumor pieces ($1\times1\times1$ mm^3) were inserted subcutaneously into the right flank of halothane-anesthesized 6 weeks old BALBc nu/nu mice. After ~3 weeks, animals with a tumor volume (TV) of 100 mm^3 were selected and divided into three groups of five mice each. TV was assessed by using a caliper measuring the two major diameters by the formula $TV = \pi/6\ (d1\times d2)^{1/2}$. Treatment was started at a TV of ~300 mm^3. For comparing wild-type endostatin with mutant endostatin with no Zn binding, mice were treated with recombinant human endostatin (hES) or the double deletion mutant (ΔNΔC) with each mouse receiving 10 μg/kg/day subcutaneously around the tumor for 4 days. TV was measured at two time points before the start of treatment and at the start of treatment to determine the growth rate of the tumors. TV was also measured 2 and 4 days after treatment. On the fourth day after treatment the blood was taken by heart puncture for biochemical analysis and animals were killed. Serum calcium and phosphate were determined by automated autoanalyzer techniques. The concentration of 10 μg/kg/day was chosen based on preliminary experiments in which three doses of human endostatin, 10, 50 and 250 μg/kg/day, were given by daily injections around the tumors for 17 days. TV was measured at two time points before the start of treatment, at the start of treatment, and then several times until the end of the experiment. All three doses gave a maximal tumor regression of 20–40% in the first 4–5 days of treatment.

Acknowledgements

We are grateful to Dr Noel Bouck for suggesting the use of migration assays and for the initial testing of the inhibitory effect on bFGF-induced migration of human dermal microvascular endothelial cells. We thank Dr Ute Felbor and Leena Karttunen for critical reading of the manuscript and helpful suggestions. Mrs Yulia Pittel provided expert secretarial and editorial service. The study was supported by NIH grant AR36820, a grant from EntreMed, Inc., EC grant BI04-CT96-0537, and NIH grant EY12109.

References

Boehm,T., Folkman,J., Browder,T. and O'Reilly,M.S. (1997) Antiangiogenic therapy of experimental cancer does not induce acquired drug resistance. *Nature*, **390**, 404–407.

Boehm,T., O'Reilly,M.S., Keough,K., Shiloach,J., Shapiro,R. and Folkman,J. (1998) Zinc-binding of endostatin is essential for its antiangiogenic activity. *Biochem. Biophys. Res. Commun.*, **252**, 190–194.

Dhanabal,M., Ramchandran,R., Volk,R., Stillman,I.E., Lombardo,M., Iruela-Arispe,M.L., Simons,M. and Sukhatme,V.P. (1999) Endostatin: yeast production, mutants and antitumor effect in renal carcinoma. *Cancer Res.*, **59**, 189–197.

Ding,Y.H. *et al*. (1998) Zinc-dependent dimers observed in crystals of human endostatin. *Proc. Natl Acad. Sci. USA*, **95**, 10443–10448.

Halfter,W., Dong,S., Schurer,B. and Cole,G.J. (1998) Collagen XVIII is a basement membrane heparan sulfate proteoglycan. *J. Biol. Chem.*, **273**, 25404–25412.

Hohenester,E., Sasaki,T., Olsen,B.R. and Timpl,R. (1998) Crystal structure of the angiogenesis inhibitor endostatin at 1.5 Å resolution. *EMBO J.*, **17**, 1656–1664.

Kohfeldt,E., Maurer,P., Vannahme,C. and Timpl,R. (1997) Properties of the extracellular calcium binding module of the proteoglycan testican. *FEBS Lett.*, **414**, 557–561.

Mayer,U., Nischt,R., Poschl,E., Mann,K., Fukuda,K., Gerl,M., Yamada,Y. and Timpl,R. (1993) A single EGF-like motif of laminin is responsible for high affinity nidogen binding. *EMBO J.*, **12**, 1879–1885.

Muragaki,Y., Timmons,S., Griffith,C.M., Oh,S.P., Fadel,B., Quertermous,T. and Olsen,B.R. (1995) Mouse *Col18a1* is expressed in a tissue-specific manner as three alternative variants and is localized in basement membrane zones. *Proc. Natl Acad. Sci. USA*, **92**, 8763–8767.

O'Reilly,M.S. *et al*. (1997) Endostatin: an endogenous inhibitor of angiogenesis and tumor growth. *Cell*, **88**, 277–285.

Oh,S.P., Kamagata,Y., Muragaki,Y., Timmons,S., Ooshima,A. and Olsen,B.R. (1994a) Isolation and sequencing of cDNAs for proteins with multiple domains of Gly-X-Y repeats identify a novel family of collagenous proteins. *Proc. Natl Acad. Sci. USA*, **91**, 4229–4233.

Oh,S.P., Warman,M.L., Seldin,M.F., Cheng,S.-D., Knoll,J.H., Timmons,S. and Olsen,B.R. (1994b) Cloning of cDNA and genomic DNA encoding human type XVIII collagen and localization of the α1(XVIII) collagen gene to mouse chromosome 10 and human chromosome 21. *Genomics*, **19**, 494–499.

Pöschl,E., Mayer,U., Stetefeld,J., Baumgartner,R., Holak,T.A., Huber,R. and Timpl,R. (1996) Site-directed mutagenesis and structural interpretation of the nidogen binding site of the laminin γ1 chain. *EMBO J.*, **15**, 5154–5159.

Rehn,M. and Pihlajaniemi,T. (1995) Identification of three N-terminal ends of type XVIII collagen chains and tissue-specific differences in the expression of the corresponding transcripts. The longest form contains a novel motif homologous to rat and *Drosophila* frizzled proteins. *J. Biol. Chem.*, **270**, 4705–4711.

Saarela,J., Rehn,M., Oikarinen,A., Autio-Harmainen,H. and Pihlajaniemi,T. (1998) The short and long forms of type XVIII collagen show clear tissue specificities in their expression and location in basement membrane zones in humans. *Am. J. Pathol.*, **153**, 611–626.

Sasaki,T., Fukai,N., Mann,K., Gohring,W., Olsen,B.R. and Timpl,R. (1998) Structure, function and tissue forms of the C-terminal globular domain of collagen XVIII containing the angiogenesis inhibitor endostatin. *EMBO J.*, **17**, 4249–4256.

Vallejo,A.N., Pogulis,R.J. and Pease,L.R. (1994) *In vitro* synthesis of novel genes: mutagenesis and recombination by PCR. *Genome Res.*, **4**, S123–S130.

Weissglas,M., Schamhart,D., Lowik,C., Papapoulos,S., Vos,P. and Kurth,K.H. (1995) Hypercalcemia and cosecretion of interleukin-6 and parathyroid hormone related peptide by a human renal cell carcinoma implanted into nude mice. *J. Urol.*, **153**, 854–857.

Weissglas,M.G., Schamhart,D.H., Lowik,C.W., Papapoulos,S.E., Theuns,H.M. and Kurth,K.H. (1997) The role of interleukin-6 in the induction of hypercalcemia in renal cell carcinoma transplanted into nude mice. *Endocrinology*, **138**, 1879–1885.

Yoshida,A., Anand-Apte,B. and Zetter,B.R. (1996) Differential endothelial migration and proliferation to basic fibroblast growth factor and vascular endothelial growth factor. *Growth Factors*, **13**, 57–64.

Received April 15, 1999; revised and accepted June 22, 1999